Journal of Earth Science, Vol. 36, No. 4, p. 1766–1779, August 2025 *ISSN 1674-487X*
Printed in China
https://doi.org/10.1007/s12583-024-0099-8

Characteristics of Channel Sand Body Based on 3D Digital Outcrop Model: A Case Study of Shaximiao Formation Outcrop, in Sichuan Basin, China

Xianghui Zhang[1], **Changmin Zhang**[*1], **Wei Yang**[2], **Wenjun Fu**[3], **Zhihong Wang**[2], **Qinghai Xu**[1]

1. *School of Geosciences*, *Yangtze University*, *Wuhan* 430100, *China*
2. *Research Institute of Petroleum Exploration & Development*, *PetroChina*, *Beijing* 100089, *China*
3. *Hainan Branch of CNOOC* (*China*) *Ltd.*, *Hainan* 570311, *China*

ABSTRACT: To address the shortage of characterization scale of field outcrops, we used the characteristics of unmanned aerial vehicle (UAV) oblique photography with a wide field of view and a high degree of quantification for image acquisition, data processing, and geological interpretation of the outcrops of the Shaximiao Formation in the Sichuan Basin. We established a 3D digital outcrop model (DOM), which combines the advantages of visualization and digitization the 3D DOM to interpret the characteristics of typical channel sand bodies. Within the study area, we have identified three types of channel deposition: composite channel deposition, crevasse channel deposition, and abandoned channel deposition. Among these, the composite channel deposition was mainly sandstone, the bottom contains conglomerate, with large cross-bedding, and the maximum thickness of the single sand body was 1.96 m. The crevasse channel deposition was mainly fine sandstone and siltstone, with massive bedding and small cross-bedding, and the maximum thickness of the single sand body was 0.64 m. The abandoned channel deposition dominated by mudstone with thin sandstone, the sandstone was mainly lenticular in section, and the maximum thickness of the single sand body was 0.28 m. We identified the depositional model of the studied region, which is dominated by braided river deposition, based on the growth size and correspondence of the sand bodies. The research provides a comparative foundation for the detailed characterisation of the underground reservoir sands found in the Jurassic Shaximiao Formation in the Sichuan Basin. It also serves as a reference for the effective study of UAV oblique photography technology in the field.
KEY WORDS: unmanned aerial vehicle, oblique photography, digital outcrop model, channel sand body, Shaximiao Formation, Sichuan Basin.

0 INTRODUCTION

The channel sand body served as an essential reservoir for oil and gas (Liu et al., 2004; Qiu et al., 1983; Wu et al., 1981). Conducting fine characterization studies of channel sand bodies was of great theoretical and practical significance for deepening understanding of internal reservoir architecture and remaining oil exploration (Ma X H et al., 2018; Jia C Z et al., 2012; Zou et al., 2010; Jia A L et al., 2007; Zhao et al., 2001). Geophysical techniques, modern sedimentation, flume simulation experiments, and field outcrop investigations were the main methods used to study the traditional description of the channel sand body (Jin et al., 2014; Ji et al., 2013; Zeng et al., 2012; Yu et al., 1994). The most commonly used techniques were geophysical, forward modeling, logging rock-electrical feature analysis, seismic attribute extraction analysis, and frequency division interpretation technology (Lin et al., 2013; Szarawarska et al., 2010; Cross et al., 2009; Wu et al., 2008; Yin et al., 2001). With the increase in the fine scale of sand body characterization, its characterization techniques were also improving. Among them, Fabuel-Perez et al. (2009) investigated outcrop characterisation and geostatistical analysis of a low-sinuosity fluvial-dominated succession using digital outcrop models. Sahoo and Gani (2015) Creating three-dimensional channel bodies in LiDAR-integrated outcrop characterization. Moreover, Yue et al. (2019) examined the architecture of the point bar of a meandering fluvial river using ground penetrating radar (GPR).

In recent years, with the rapid development of UAV technology and the increasing civilization, the technical research of UAV-related applications has been expanding (Hayat et al., 2016; Colomina and Molina, 2014; Ber-

*Corresponding author: yangtzeu3rg@163.com
© China University of Geosciences (Wuhan) and Springer-Verlag GmbH Germany, Part of Springer Nature 2025

Manuscript received April 28, 2024.
Manuscript accepted October 22, 2024.

Zhang Xianghui, Zhang Changmin, Yang Wei, Fu Wenjun, Wang Zhihong, Xu Qinghai, 2025. Characteristics of Channel Sand Body Based on 3D Digital Outcrop Model: A Case Study of Shaximiao Formation Outcrop, in Sichuan Basin, China. *Journal of Earth Science*, 36(4): 1766–1779. https://doi.org/10.1007/s12583-024-0099-8. http://en.earth-science.net

ni et al., 2009). 3D digital outcrop characterization technology based on UAV oblique photography has been introduced into geological field work (Marques et al., 2020; Buckley et al., 2019; Bemis et al., 2014). Chesley et al. (2017) used UAV and structure-from-motion (SfM) to characterize sedimentary outcrops in the Morrison Formation, Utah, USA. Nieminski and Graham (2017) used a small UAV and SfM to stratigraphic interpretation. Nesbit et al. (2021) used UAV and SfM to confirm and enhance previous field-based documentation of coarse-scale stratigraphic architecture in deep-water channel deposits. Compared with the traditional manual modeling method, the establishment mentioned above of these digital outcrop models has the characteristics of fast maneuverability, accuracy and efficiency, and low use cost. As a result, digital outcrops have quickly developed into an essential tool for geological interpretation. Pickel et al. (2015) built digital outcrop models with a training image. Osman et al. (2017) used the digital outcrop workflow in the sedimentological interpretation of the Early Triassic Upper Khartam Member of the Khuff Formation. Liang et al. (2022) used the digital outcrop to interpret the 3D quantitative characterization of fractures and cavities. 3D digital outcrop models based on UAV oblique photography technology has become a hot spot for research and application (Zhang et al., 2020; Yan et al., 2019; Yin et al., 2018).

The Jurassic Shaximiao Formation in the Sichuan Basin is a tropical desert seasonal fluvial deposit that is part of the Mesozoic red layer. It is composed of interbedded orthoclase sandstone, feldspathic quartz sandstone, and mudstone (Xia et al., 1984). Dinosaur fossils have been found within the formation (Moore et al., 2020). Field observation, core description, log phase analysis, and seismic interpretation were used by Yang et al. (2014) to investigate the sedimentary characteristics of the Shaximiao Formation in Northwest Sichuan. Liu et al. (2018) conducted a study of the Jurassic sedimentary system in the Sichuan Basin, utilizing field outcrop and core data. Their findings indicate that the Shaximiao Formation was the primary site of the development of four sedimentary facies types of the alluvial fan-fluvial-delta-lake sedimentary system. Yu et al. (2019) determined that the Jurassic Shaximiao Formation of the Longmen Mountain frontal zone in West Sichuan developed two sedimentary facies: alluvial fan and braided river delta, based on field outcrop sections. Based on sedimentation analysis, the sand body characteristics of the Shaximiao Formation show a narrow channel in general, a highly irregular spatial distribution of the sand body (Fang et al., 2023), complex lithologic interface morphology, and complex channel superposition (Fan, 2022). The information aspects revealed by the subsurface geological interpretation and the two-dimensional photographs of the outcrop are the primary focus of these research. Nevertheless, because of the Sichuan Basin's high and steep terrain and the manual camera's lack of viewing angle. It is difficult to consider the outcrop architecture in a realistic, intuitive, and complete manner. Meanwhile, there is a serious issue with various interpretations with subsurface geological interpretation. Consequently, the depositional environment of the Shaximiao Formation is a subject of varying interpretations among academicians (Zhang et al., 2022; Liu et al., 2018). The study used the 3D digital outcrop model characterization technique of UAV oblique photography for fieldwork research, which has established the 3D digital outcrop model in Shaximiao Formation, Sichuan Basin. Our research refined the characteristics of the channel sand body through 3D visualization analysis to deepen the understanding of the internal geological architecture. The result provides a comparative foundation for the detailed characterization of the underground reservoir sands found in the Jurassic Shaximiao Formation in the Sichuan Basin. It also serves as a reference for the effective study of UAV oblique photography technology in the field. The study used the 3D digital outcrop model characterization technique of UAV oblique photography for fieldwork research, which has established the 3D digital outcrop model in Shaximiao Formation, Sichuan Basin. Through 3D visualisation analysis, our research improved the geological architecture by analysing the characteristics of the channel sand body. The findings provide a basis for comparison that will be useful in characterising the underground reservoir sands in the Jurassic Shaximiao Formation of the Sichuan Basin in detail. It may also be used as a reference for conducting an efficient field research of UAV oblique photography technology.

1 BACKGROUND

Sichuan Basin was located on the western margin of the ancient Yangzi Plate and was a multi-cycle superimposed basin developed from the Upper Yangtze Craton. Since the Middle Triassic, the Sichuan Basin has been influenced by the Indonesian Movement, Yanshanian, and the Himalayan movements, forming the present tectonic framework (Wang et al., 2014; Chen et al., 1994). The Sichuan Basin was mostly bordered by the Longmenshan fold belt, Daba Mountain fold belt, and Micang Mountain uplift belt, forming a diamond-shaped configuration. The direction of the basin was northeast. The basin area was 19×10^4 km^2 (Figure 1a), and this research specifically examines the Jurassic Shaximiao Formation located in the Sichuan Basin.

The Jurassic Shaximiao Formation was the least deeply buried formation containing hydrocarbons compared to other formations in the Sichuan Basin. The formation may be divided into the Lower Shaximiao Formation and the Upper Shaximiao Formation (Figure 1c). During the deposition of the middle and upper sections of the Lower Shaximiao Formation, the lake water in the study region completely receded. In the northern half of the basin, fluvial processes predominate, and the predominant lithology consisted of purple-red mudstone with light gray

sandstone. During the last stage of the Lower Shaximiao Formation, the basin had a transient period of sedimentation in a shallow lake environment. Nevertheless, the duration was quite brief, and the fluvial characteristics were reinstated. Throughout the Upper Shaximiao Formation, the basin was primarily characterized by a highly oxidized sedimentary environment and saw the development of fluvial facies until the deposition of the Shaximiao Formation concluded. The Upper Shaximiao Formation is composed of thick floodplain mudstone that is mostly purple-red in color, interspersed with channel sand bodies that exhibit shades of gray and gray-green (Zhang et al., 2022).

The study area was located in the northeastern part of the Sichuan Basin, between E107°36′36″–E107°43′48″ and N30°32′42″–N30°36′18″, in He Lin Town, Liangping District, Chongqing (Figure 1b). The general orientation of the mountain was NE direction, which was consistent with the basin orientation. In this area, the Shaximiao Formation was tectonically buried to a depth of -2 000 – -3 000 m (Duan, 2021; Wen et al., 2005) and exhibited a widely distributed channel sand body from the basin margin to the interior, providing the main reservoir for the Shaximiao Formation. However, the steep topography of the basin makes the traditional field description relatively difficult. In order to interpret the sandstone deposition pattern of the Shaximiao Formation, this paper uses UAV scanning in this study area to establish a 3D digital model, which in turn facilitates the interpretation of the sedimentary phase and sandstone prediction.

2 DATA AND METHODS

2.1 Oblique Images Acquired

The oblique photogrammetry technology uses multi-angle cameras to acquire high-resolution aerial images of ground objects from all angles simultaneously. This technology expands the application range of remote sensing images and changes the traditional way of collecting images only from the frontal camera angle. The 3D model produced using oblique photogrammetry technology can genuinely reflect the scene that conforms to the human eye vision. It combines the GNSS (GPS + GLONASS + GALILEO) technology with DJI UAV to incorporate the 3D outcrop into the geographic information framework, showing comprehensive and rich geographic information (Table 1). The study used the DJI Air 2S multi-rotor UAV. The UAV platform can be controlled from -90° to 24° (pitching) and takes a camera with 20 megapixels, which can meet the field's multi-angle and high-precision image acquisition.

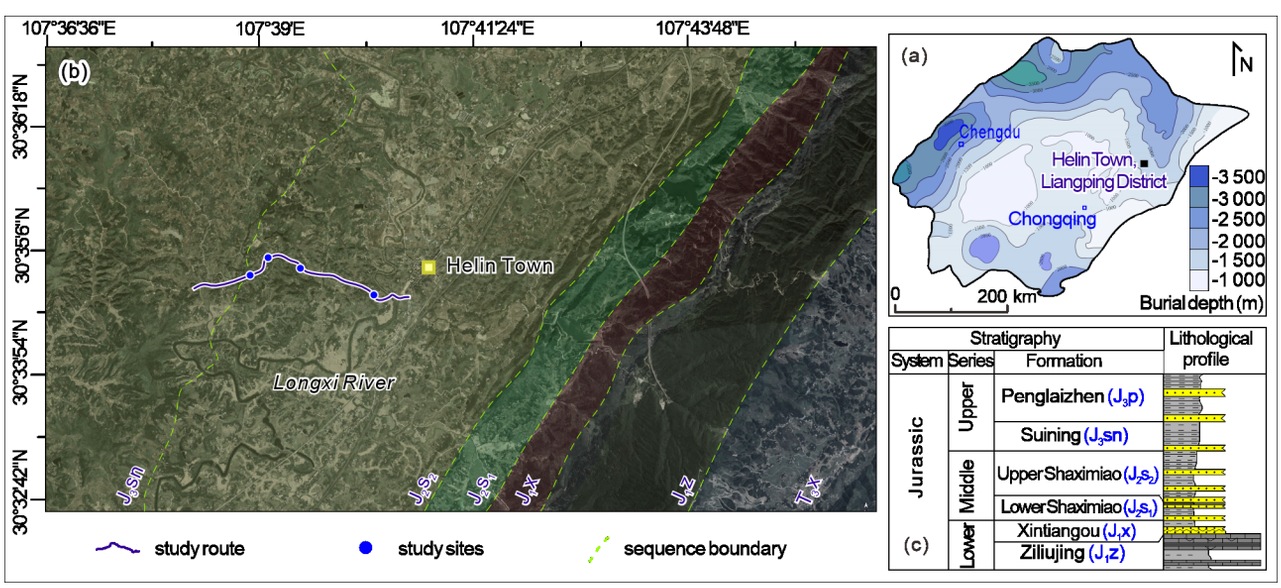


Figure 1. Regional geological background. (a) The study area was located in the Sichuan Basin, southwestern China, and the outcrop location is in He Lin Town, Liangping District, Chongqing. The buried thickness of the Shaximiao Formation is about -1 500– -2 000 m. (b) Stratigraphic boundaries and fieldwork observation points in the study area, including four sites in total. (c) Lithological characteristics of each stratum exposed in the study area.

Table 1 Digital information acquisition of lithology at each section based on UAV oblique photography, including total area of the section at each observation point, areas of different lithologies, and maximum sandstone thickness

Position	Total area (m^2)	Sand area (m^2)	Mud area (m^2)	Maximum single sand body thickness (m)	Sandstone area/total area
P1	157.49	148.87	8.62	1.96	0.95
P2	143.66	40.37	103.29	0.64	0.28
P3	72.63	11.36	61.27	0.28	0.16
P4	334.43	136.51	197.92	0.57	0.41

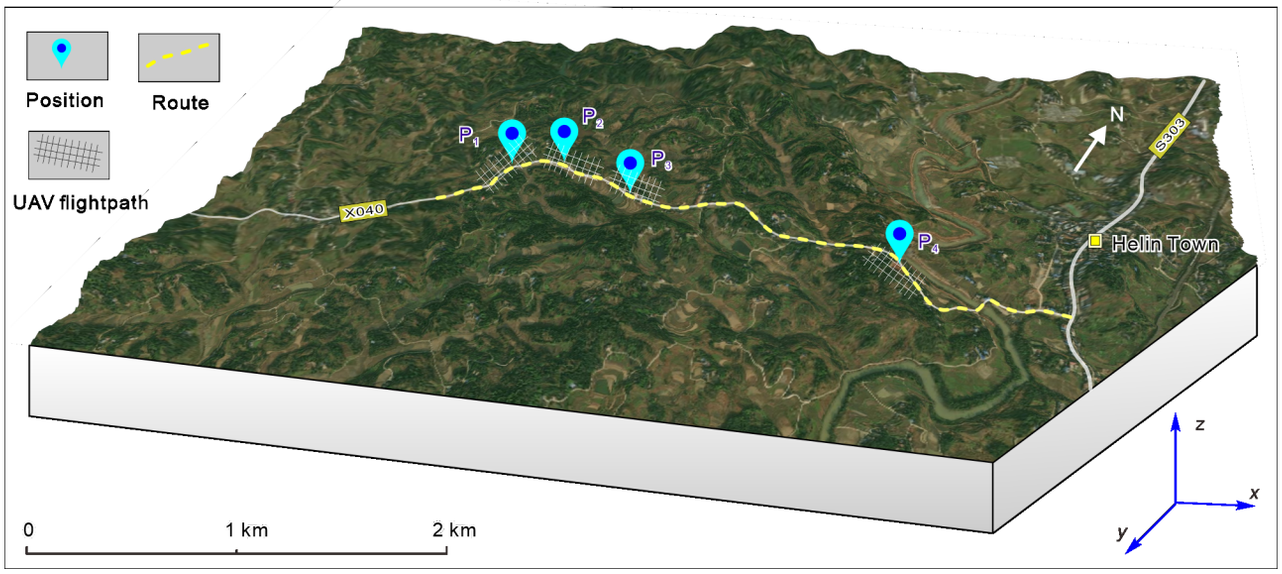


Figure 2. UAV cruise routes in the study area, with the study route following Rural Road 040. A total of four specific UAV oblique photography sites were included, and specific cruise routes were designed for each observation site by outcrop orientation.

In data acquisition, our information includes traditional manual detailed investigation and UAV oblique photography. Among them, in the UAV photography data acquisition, we designed two flight heights according to the topographic and geomorphological features. In the key outcrop area, we designed a flight altitude of 10 m. Combined with the capabilities of the camera, the resolution of the profile can be calculated to be about 1 cm according to Eq. (1). In the non-focused outcrop area, we designed the flight altitude to be 100 m, and the resolution of the profile can be calculated to be about 10 cm according to Eq. (1). These two altitudes can satisfy the integrity of the outcrop area but can also carry out fine and quantitative research on the rock layers of the key profile. According to these two flight altitudes, we accumulated 49 UAV photos at point 1, 54 UAV photos at point 2, 57 UAV photos at point 3, and 41 UAV photos at point 4 (Figure 2).

$$H = f \times (GSD/a) \quad (1)$$

H is the UAV altitude (m); f is the lens focal length (mm); GSD is the ground resolution (m); a is the pixel size (mm).

2.2 3D Modeling of Digital Outcrops

Digital outcrop modeling effectively combines UAV technology and oblique photography technology to generate a realistic 3D model and achieve 3D measurability. Our research used ContextCapture software for the study area of 3D modeling. Its modeling process mainly includes oblique photography, automatic modeling, and automatic mapping. In this study, continuous 2D images can be used to restore the accurate 3D model. Compared with manual modeling, automatic modeling of oblique photography has the advantages of high efficiency, high accuracy, high realism, and low cost (Figure 3).

3 RESULTS

Through literature research and field outcrop investigation, the study determined that the Jurassic Shaximiao Formation in the Sichuan Basin mostly consisted of deposits from fluvials and shallow lakes. Based on the UAV 3D digital outcrop model, we have discovered three different types of fluvial deposits in the research area: composite channel deposits, crevasse channel deposits, and abandoned channel deposits. Furthermore, we use the 3D model visualisation capability to classify the stages of channel erosion and the filling process in the designated research region.

3.1 Composite Channel Sand Body

The main characteristics of channel deposition were sandstone and conglomerate. Moreover, it was rich in bedding types. The cross-section was trough-shaped, and the rocks were primarily lenticular. The flushing of flowing water shows an apparent erosion surface at the bottom of the channel bed, which constitutes the base of the channel deposition unit.

The outcrop of Observation Point 1 was located at 30°35'1.12"N, 07°39'7.12"E, an orientation of 37°, and in the 3D model, the section outcrop length was about 45.52 m, and thickness was 4.76 m. The sandstone was significantly developed in the full section (Figures 4, 5), the broad sandstone area to section area ratio reaches 94.52%, and the maximum single sand body thickness reaches 1.96 m. In the front view of the 3D model, the section consists of two bottom-up normal gradings superimposed, and the change of lithologic combination mainly causes the normal grading characteristics.

A clear erosional surface was visible at the section's bottom of the single-stage channel. The lower part of the erosion surface was mainly mudstone with a thin layer of overbank sandstone, and many wormholes were devel-

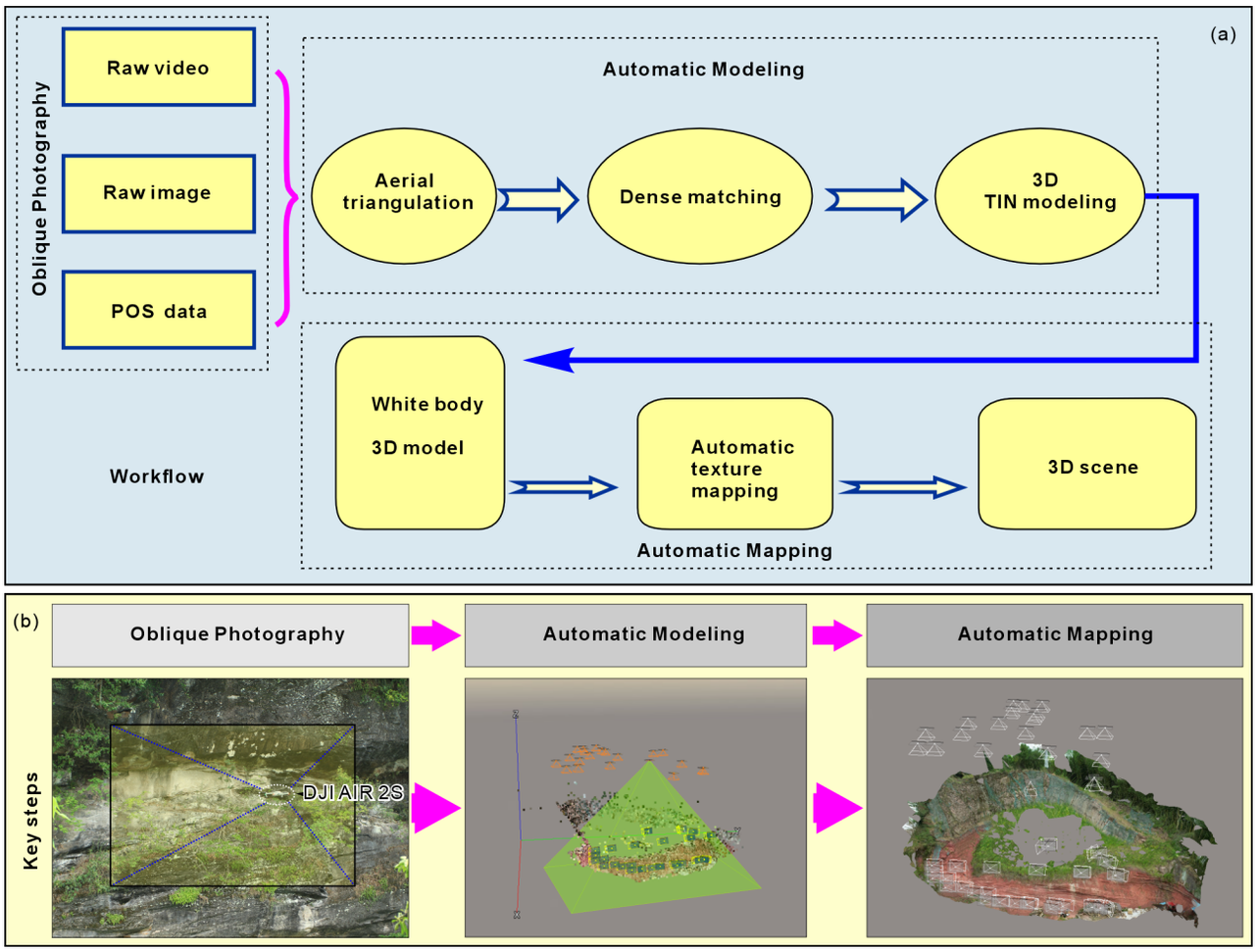


Figure 3. 3D digital outcrop modeling workflow (a), and key steps (b). Mainly consisting of three steps: UAV oblique photography, automatic modeling, and automatic mapping.

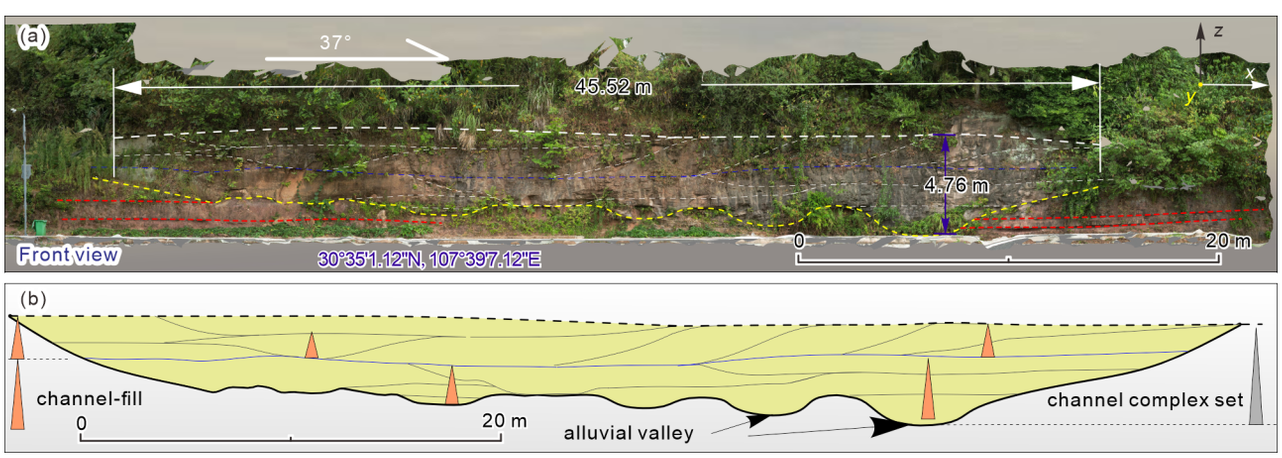


Figure 4. 3D digital outcrop characteristics of the composite channel sand body of the Jurassic Shaximiao Formation, (a) digital outcrop model front view of the sand body extensions, (b) detailed carving of the internal architecture of composite channel sand body.

oped in the sandstone. The maximum thickness of overbank sandstone was 0.32 m, and the total area of overbank sandstone was 9.01 m^2, accounting for 5.72% of the total area of the section. Obvious alluvial valleys were visible near the erosion surface, and the sediments were dominated by gravelly sandstone, with evident channel bed lag deposits visible. Upward the erosion surface, the mud clasts can be seen, the large scale cross-bedding was developed, and the sediment has obvious lower coarse and upper fine cyclothem (Figure 5). We analyzed this outcrop section's bottom-up depositional characteristics and mapped the sandstone deposition relation-

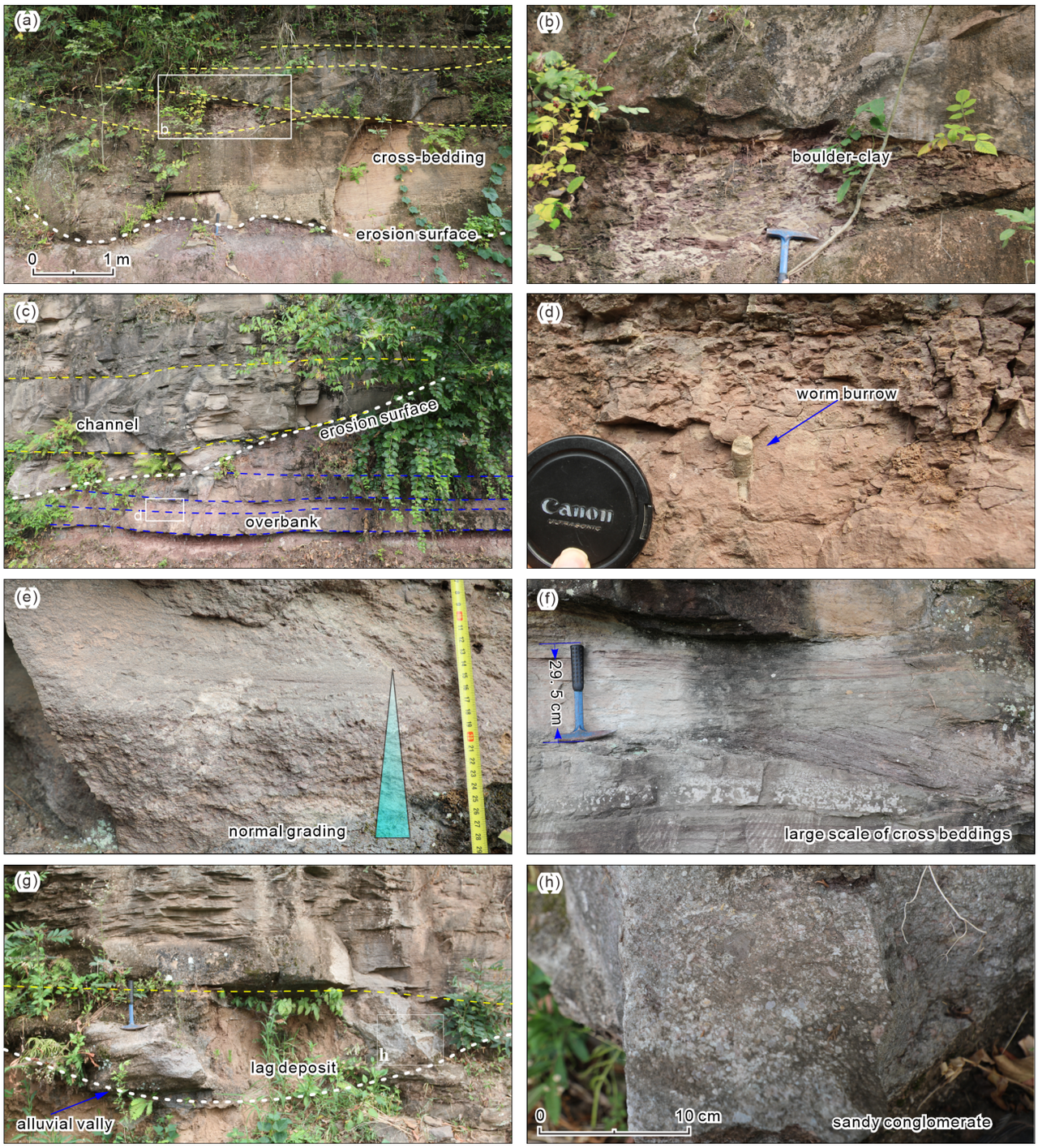


Figure 5. Interpretation of typical phenomena in composite channel sands. (a) Erosion surface visible at the bottom of the channel; (b) mud clasts; (c) the layers at the bottom of the channel show banded sandstone interspersed with mudstone; (d) wormhole; (e) normal grading; (f) large scale of cross-bedding; (g) lag deposits; (h) bottom lagging deposits exhibiting sandy conglomerate

ship under the 3D model visualization conditions. It was concluded that the section consistent with the typical channel sand characteristics and composite channel sand formed by multiple stages of sand bodies depositing on top of each other.

3.2 Crevasse Channel Sand Body

The Crevasse channel sand body was mainly formed when the flood water flows out of the main channel through a local break. The lithology was mainly fine sandstone and siltstone, with massive bedding, small cross-bedding, wave cross-bedding, and horizontal bedding. The thickness of the sand body deposited in a single crevasse channel was mostly tens of centimeters to several meters, and the rock was tongue-shaped, thinning and pinching out toward the flood plain, and the section was lenticular. When a flood loaded with sediment overflows the channel banks, sheet-shaped overflow

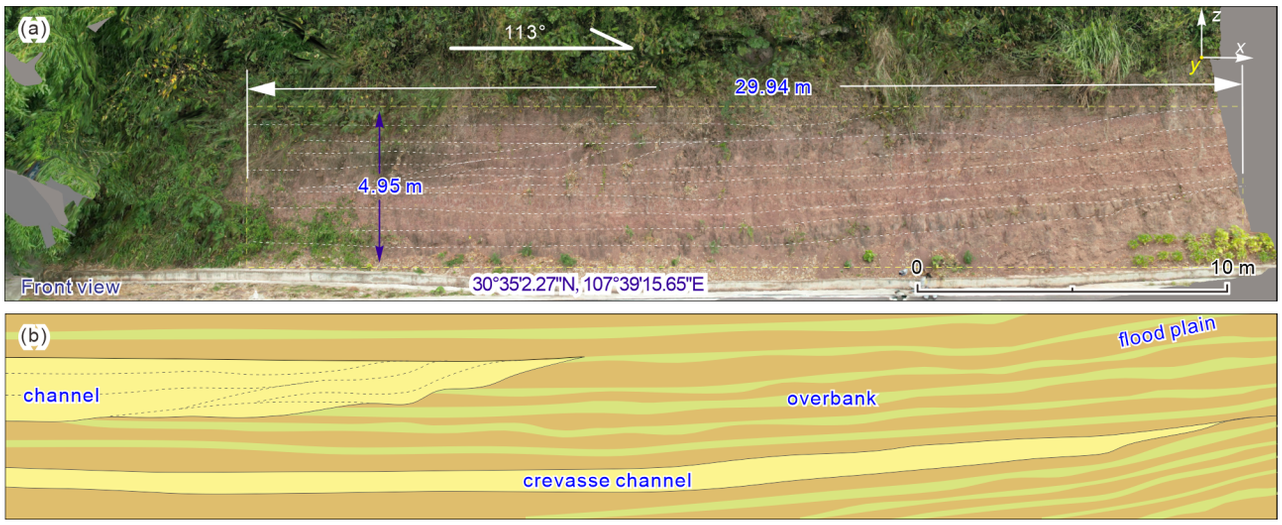


Figure 6. 3D digital outcrop characteristics of the crevasse channel sand body of the Jurassic Shaximiao Formation. (a) Digital outcrop model front view of the sand body extensions; (b) detailed carving of the internal architecture of crevasse channel sand body.

sandstone was formed on the floodplain instead of breaking the banks.

The outcrop of observation point 2 was located 30° 35'2.27"N, 107° 39'15.65"E, orientation 37° . In the 3D model, the section outcrop length was about 29.94 m, and the thickness was 4.95 m. The whole section mainly composed of mudstone (Figures 6, 7), the overall sandstone area to section area ratio only 28.10%, the sandstone content was less, and the maximum single sand body thickness was only 0.64 m. On the 3D model front view, the overall appearance was multi-stage layered mudstone with thin sandstone. The sandstone was lenticular in the cross direction, showing the typical sedimentary characteristics of the crevasse channel. The area of the crevasse channel was 8.41 m^2, accounting for 5.85% of the total area of the section, in which the maximum thickness of the sandstone of the crevasse channel was 0.43 m. There are also thin layers of overbank sandstone between the mudstone, the maximum thickness of overbank sandstone was 0.08 m, the thickness was thin but widely distributed, and the total area was 17.67 m^2, accounting for 12.30% of the total area of the section.

Unlike the typical channel depositional characteristics of Observation Site 1, the crevasse channel sand body and the overbank sand body were relatively thin, and the scale of the laminae was relatively small, mainly showing massive bedding and small cross-bedding. As the whole Jurassic Shaximiao Formation sedimentary background was an arid environment, sediment injection was visible in the mudstone (Figure 7). When the next stage of the flood loaded with sediment overflows the bank, its cracks were filled with sediment and form sandstone dikes vertical to the horizon. Above the outcrop channel, a thick layer of channel sand was developed, the sand body has a clear sequence surface, and the sandstone area was 14.29 m^2, which accounts for 9.95% of the total area of the section.

3.3 Abandoned Channel Deposits

Abandoned channel deposits consist mainly of siltstone and mudstone, and horizontal bedding was developed in the rock. On a larger scale, channel abandonment was mainly caused by redirections or crevasses. The river channel swings across the floodplain, accompanied by ephemeral streams, forming new channels in relatively low floodplain basins, while the original old channels were abandoned, and floodplains were formed around the old channels. Furthermore, a thin layer of overbank sandstone may be formed during the channel swing on the floodplain.

Observation point 3 outcrop was located at 30° 34'56.67"N, 107° 39'26.44"E, orientation 37° . In the 3D model, the section outcrop length was about 18.74 m, and the thickness was 4.72 m. The whole section was also mainly dominated by mudstone (Figures 8, 9), the overall sandstone area to section area ratio was 15.64%, and the maximum single sand body thickness was 0.28 m. On the front view of the 3D model, the bottom of the section shows multiple periods of thick mudstone interbedded with thin sandstone. In the middle of the section, obvious channel pinching was observed, and the channel filling was mainly mudstone deposits with thin sandstone. At the same time, the upper part of the section was mainly lenticular sandstone.

Similar to the thinly bedded overbank sandstone at observation site 2, the sandstone interbedded with thick mudstone in the lower part of this section shows typical floodplain and overbank sand deposition. While in the central part of the section, the muddy sediments dominate the channel, mainly typical abandoned channel deposition (Figure 9). This type of deposition may be mainly influenced by ephemeral streams, which formed a typical channel deposition section in the vertical direction during the flood period due to the erosion of the channel, while a floodplain surrounded the former channel due to the sudden abandonment of the channel. The abandoned

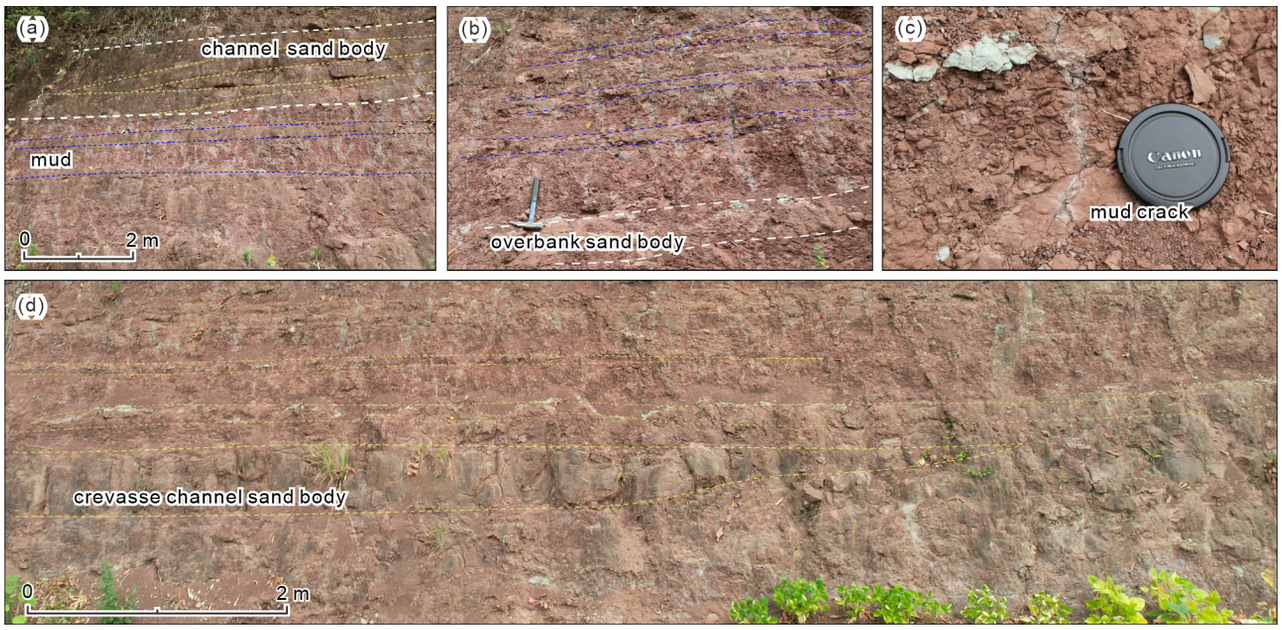


Figure 7. Observation 2 Interpretation of typical phenomena. (a) Channel sand body characteristics and internal architecture; (b) overbank sand body; (c) sediment injection; (d) crevasse channel sand body.



Figure 8. 3D digital outcrop characteristics of the abandoned channel deposits of the Jurassic Shaximiao Formation. (a) Depositional characteristics of the front view of the section;(b) sediment injection; (c) floodplain and overbank.

channel depositional characteristics differ from the typical channel-fill depositional characteristics at observation point 1. The internal filling characteristics were similar to floodplain deposition, sediment injection form the dikes, and a thin layer of overbank sandstone interbeds the thick mudstone layer.

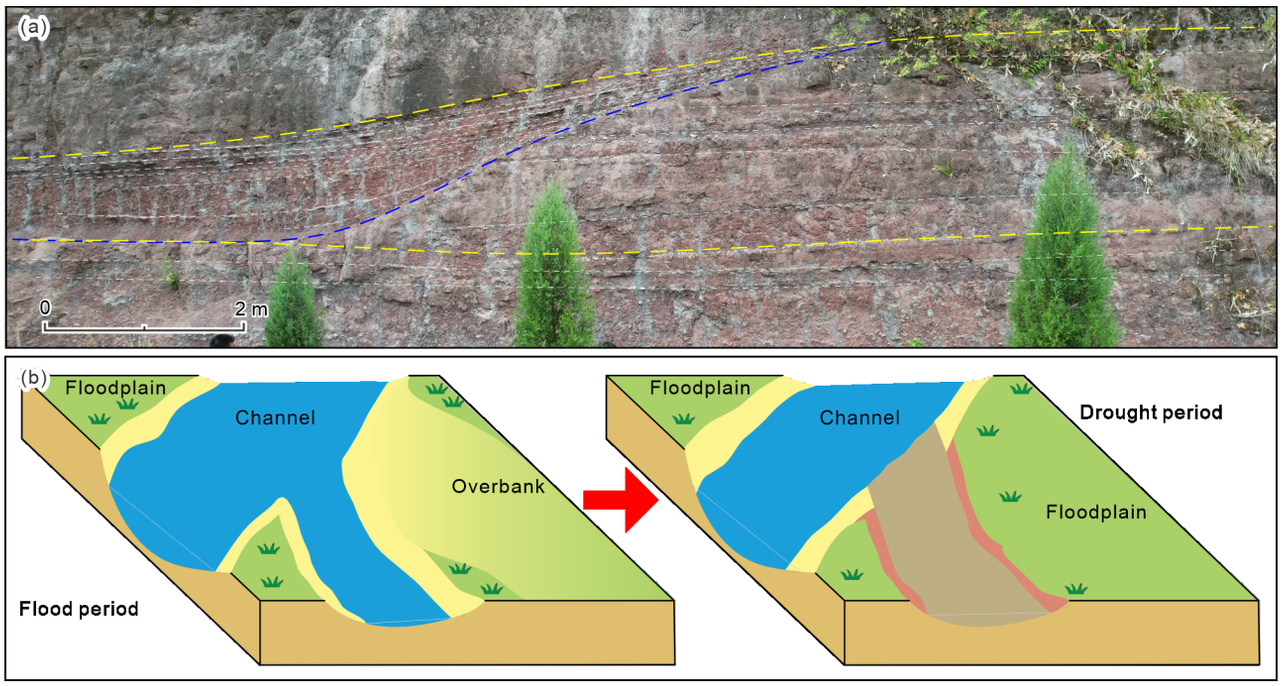


Figure 9. Observation 3 Typical phenomena. (a) Abandoned channel fill section characteristics; (b) river abandonment fill process.

3.4 Channel Erosion and Filling Process

As an essential mode of sediment transport, the channel can cause erosion, transport, and accumulation of sediment. Among them, the flowing water erodes the channel bed material and makes the channel deepen and widen; meanwhile, the sediment transported by the river can be carried downstream by suspension, saltation, and rolling. Influenced by the change of hydrodynamic conditions, the sediment accumulates on the channel bed and forms the channel filling, and this whole process belongs to one deposition event. When the next depositional event occurs, the previous stage of channel filling was accompanied by a new stage of erosion, transport, and accumulation, forming the next stage of channel filling. This cycle repeats itself, and the entire process of continuous channel erosion and filling can be observed on the outcrop.

Observation point 4 outcrop was located at 30° 34'42.13"N, 107° 40'14.43"E, orientation 322°, and in the 3D model, the section outcrop length was approximately 71.71 m, and thickness was 22.96 m. This section differs from the previous three observations. The section can be observed as triangular in the plan through the vertical view angle. In the side view direction, the sedimentary characteristics of the three sections can be observed. Based on the lithological characteristics of the Jurassic strata in the Sichuan Basin, it was considered that the sandstone of the Suining Formation was in the upper part of this outcrop, with an outcrop height of about 11.61 m. The lower part was the Shaximiao Formation, represented by the typical red layer of the target layer, with an outcrop height of about 11.35 m (Figure 10). Based on the 3D digital outcrop, the sequence boundary of the formation can be classified by multi-angle observation.

In the front view of the target layer, it can be observed that the section has an apparent stage subordination from bottom to top. The lower part of this section mainly shows a thick layer of mudstone interbedded by a thin layer of overbank sandstone, the maximum thickness of overbank sandstone was 0.26 m. The total area of overbank sandstone was 56.42 m^2, accounting for 16.87% of the total area of the section (Figure 10). It was similar to the overbank sandstone and flood plain depositional characteristics of observation site 2. The upper part of the section shows typical channel deposition. The maximum sandstone thickness was 0.57 m, the total area of sandstone was 80.09 m^2, accounting for 23.94% of the total area of the section, and a clear channel erosion surface can be observed. Its overall thickness was about 2.36 m, and three stages of obvious channel deposition events were classified at this site based on the identified erosion surfaces. Furthermore, the three stages of channel erosion filling types were further summarized based on how the erosion surfaces cut each other (Figure 11).

4 EXPLANATIONS AND DISCUSSIONS

The channel sediments in the study area have coarse grain size, frequent lateral migration of the river, and apparent vertical superposition. A set of upward from coarse to fine sequence ends, followed by another coarse to fine layer sequence, which has been repeated many times, constituting a multi-stage channel superposition style. This multi-stage channel superposition style was mainly caused by frequent changes in stream flow, constant migration and redirection, and multiple erosion. The channels were superimposed laterally and vertically with high width-to-depth ratios, which was suitable for braided channel deposition characteristics. Both sides of

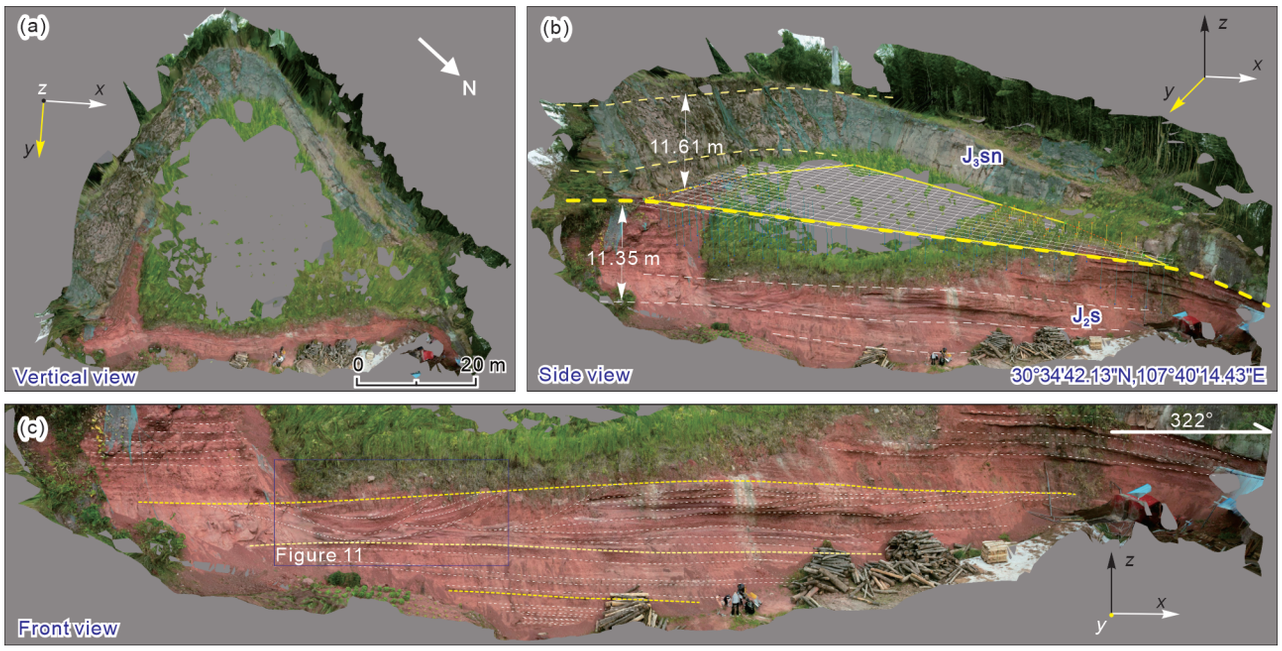


Figure 10. 3D digital outcrop characteristics of the channel erosion and filling process of the Jurassic Shaximiao Formation. (a) Front view provides an overall macroscopic description of the section location, section orientation, and section size information; (b) side view delineates the section sand body orientation as well as the section stratigraphy based on the front view; (c) front view, selected target layer, a fine description of the sandstone extension pattern of the target layer.

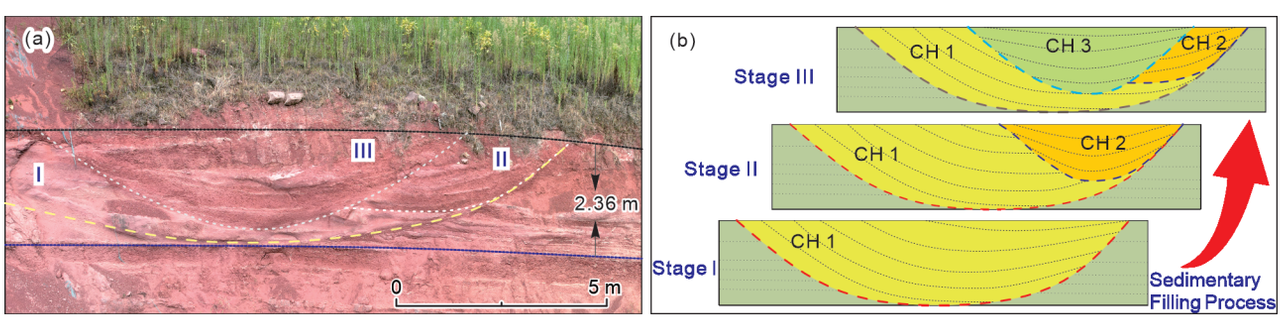


Figure 11. Digital outcrop 3D visualization of the channel stage classification. (a) Local fine detailing of the channel erosion-fill process by UAV modeling; (b) divided into three stages of channel flushing and filling process.

the channel show a transition from siltstone-dominated overbank deposition to a floodplain dominated by mudstone on the outer side. In low areas of the floodplain, during flooding, floodwaters can spill over to form small lakes on both sides of the channel (Figure 12). These small lakes were environmentally stable, biologically abundant, and can preserve complete biological remains. Traditional views interpret the sandstone of the Shaximiao Formation in the Liangping area as channel sand (Yu et al., 2019), lacking knowledge about what specific type of channel sandstone it was. In this paper, the interpretation was compared with the traditional results, and this paper clarifies the type of fluvial developed in the Shaximiao Formation in the Liangping area of East Sichuan with the assistance of the UAV 3D digital model (Figure 12).

We determined the deposition of braided channels by analyzing the depositional characteristics of outcrops in the Liangping area. Moreover, we also establish a depositional model of the Shaximiao Formation in the area (Figure 12). The study area's microscopic analysis of sedimentary characteristics of typical channels was achieved by establishing 3D digital outcrops. Its analysis consists of two main parts. The first part was the vertical staging of channel deposition, which includes identifying a single channel and classification of the stages of the composite channel. The second part was the lateral boundary classification. With the advantage of 3D digital outcrop model visualization, reasonable lateral boundary delineation was carried out based on vertical staging. Combined with the previous knowledge of the depositional environment of the Shaximiao Formation, as well as based on this three-dimensional model, the microanalysis of the sand body expands in the study area was completed.

The anatomical results show that the maximum single sandstone thickness in each digital outcrop section was still dominated by channel sand (Figure 13). The

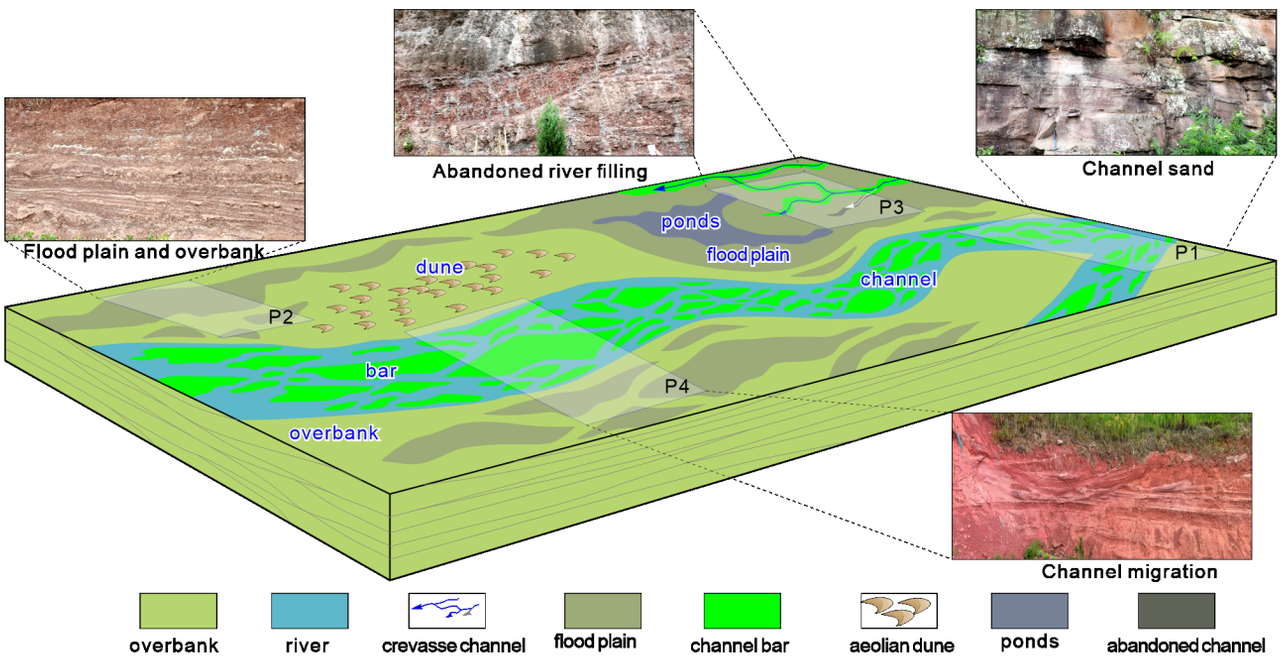


Figure 12. Deposition model of the Shaximiao Formation in the Liangping area of the Sichuan Basin based on the UAV 3D digital outcrops.

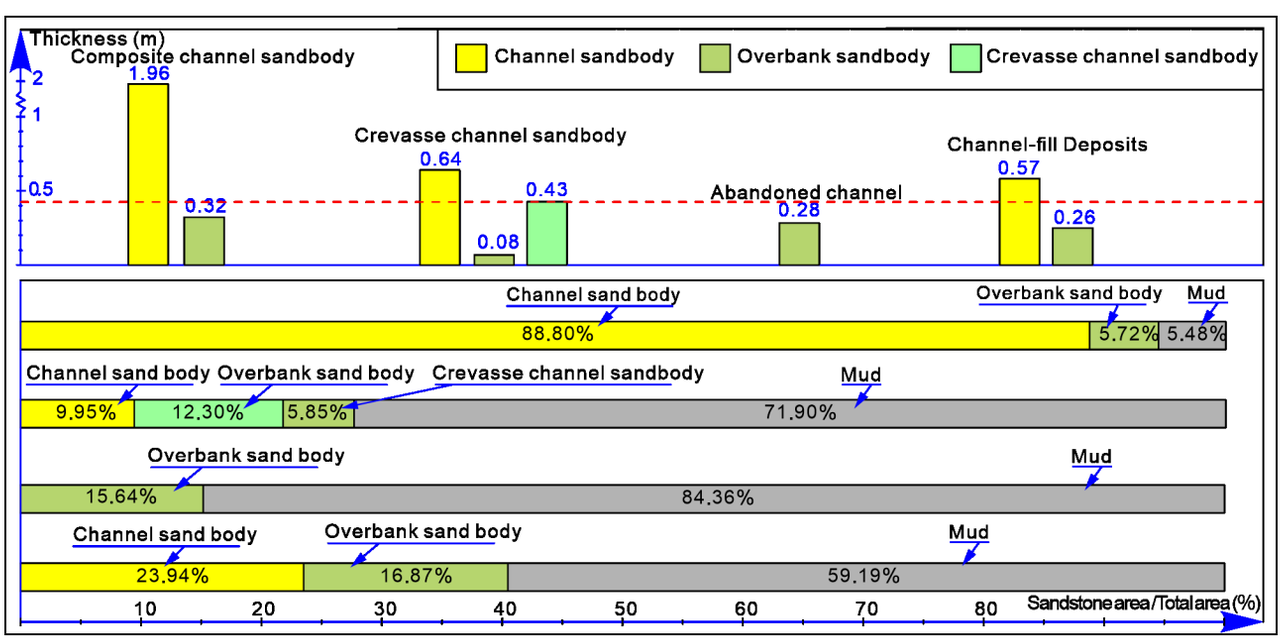


Figure 13. Maximum single sand body thickness and proportion of various types of sand bodies in the sections of the Shaximiao Formation in the Liangping area.

maximum single sandstone thickness in the composite channel of observation point 1 reaches 1.96 m, which was a good place for oil and gas reservoir in the Shaximiao Formation and was proved by actual production in the current exploration and development process (Huang et al., 2017; Wang et al., 2004). The sand body of the crevasse channel at observation point 2 was much larger than the thickness of the overbank sandstone. However, of the different types of sandstone, the overbank sandstone accounts for 12.3% of the entire section, which was more than twice the area of the sand body of the crevasse channel (5.85%). In addition, the overbank sandstone was also developed in the abandoned channel at observation points 3 and 4, accounting for 15.64% and 16.87% of the entire section, which was a widely distributed sandstone type in the study area (Figure 13).

The Jurassic Shaximiao Formation in the Sichuan Basin was rich in natural gas resources (Dai et al., 2012) and has produced more than 30 × 10^8 m^3 of gas cumulatively (Duan, 2021; Liang et al., 2011). For the high-quality reservoir, accurate evaluation was the critical point at present (Ma Y S et al., 2018; Du et al., 2014; Yang et al., 2007). The composite channel sands in this research project can be used as a preferential target for rating

high-quality reservoirs, followed by the crevasse channel sands. Moreover, the overbank sandstones in the study area can be used as a sweet spot for exploring remaining oil and gas resources (Figure 13).

In this article, we employ DOMs for the characterization of outcrop and more specifically we demonstrate how DOMs represent a powerful tool in quantification of dimensions of geobodies in outcrop. Statistical analysis and relationships of the different sandbody can be used in subsurface reservoir models of analog systems deposited in similar environments. Width-to-thickness ratios can be used to estimate body width when only the thickness is known. At the same, distribution of architectural elements and the relationship between geobodies observed in the qualitative analysis can provide valuable information to understand architecture and facies distribution of reservoirs in similar systems. Of course, digital outcrops also have certain limitations. It is still necessary to manually survey and supplement relevant information in areas with severe weathering or in environments with severe vegetation coverage.

5 CONCLUSIONS

The use of UAV oblique photography in outcrop work has changed the workflow and methods of traditional outcrops. We can use UAV measurement and mapping. The section's geomorphic characteristics and sedimentary information were concentrated in a 3D digital outcrop model. It was a more comprehensive, intuitive, and realistic way to reflect the section's sequence of layers, structures, and sedimentary characteristics compared with the traditional 2D image information.

Three types of channel deposition were identified in the study area: composite channel deposition, crevasse channel deposition, and abandoned channel deposition. In addition to the typical channel deposition characteristics of these three channel deposits on a large scale, there were also significant differences in the fine characterization processes on a small scale. The typical characteristic was the significant difference in lithology between the abandoned channel deposits and the other two channel deposits, where the abandoned channel deposits were dominated by mudstone with thin sandstone, the sandstone was mainly lenticular in section, and the maximum thickness of single sand body was 0.28 m. In contrast, the composite channel sand and the crevasse channel sand were dominated by sandstone. Although the lithology of the composite channel deposition was similar to the crevasse channel deposition, there were apparent differences in the scale of sedimentary structures. The crevasse channel sand body was smaller in scale and dominated by massive bedding and small cross-bedding, and the maximum thickness of single sand body was 0.64 m. The composite channel sand body was mainly characterized by large cross-bedding, and the maximum thickness of single sand body was 1.96 m.

This study provides a new method for the fine characterization of reservoir sands, which was vital for the identification of subsurface reservoir sands in the Sichuan Basin of the study area. With the advantage of 3D visualization of the digital outcrop model, it has a significant reference value for establishing the deposition model of the target area. The use of DOMs in combination with traditional field data offers significant improvements in efficiency, accuracy, and utility in outcrop characterization and provides results that can be applied to other analog studies to produce better quantified data sets and generate more representative reservoir models. Of course, the following points should also be noted when we use the UAV oblique photography technology to research. (1) The camera resolution mainly controls the accuracy of the outcrop measurement, so the accuracy of the 3D digital model we establish should also be based on the equipment itself. (2) The 3D digital outcrop was still essentially composed of an information-rich 2D image overlay. The higher the accuracy of the image overlay, the more accurate the model, but the greater the computational workload. Therefore, in the process of oblique photography, the degree of superimposition of 2D images should be balanced.

ACKNOWLEDGMENTS

This study was supported by the Natural Science Foundation of China (No. 42130813) and CNPC Innovation Fund (No. 2024DQ02-0502). We thank China National Petroleum Corporation (CNPC) for providing data and generous technical support. The authors are grateful to the reviewers for commenting on the original draft and improving the manuscript. The final publication is available at Springer via https://doi.org/10.1007/s12583-024-0099-8.

Conflict of Interest

The authors declare that they have no conflict of interest.

REFERENCES CITED

Bemis, S. P., Micklethwaite, S., Turner, D., et al., 2014. Ground-Based and UAV-Based photogrammetry: A Multi-Scale, High-Resolution Mapping Tool for Structural Geology and Paleoseismology. *Journal of Structural Geology*, 69: 163–178. https://doi.org/10.1016/j.jsg.2014.10.007

Berni, J. A. J., Zarco-Tejada, P. J., Suarez, L., et al., 2009. Thermal and Narrowband Multispectral Remote Sensing for Vegetation Monitoring from an Unmanned Aerial Vehicle. *IEEE Transactions on Geoscience and Remote Sensing*, 47(3): 722–738. https://doi.org/10.1109/TGRS.2008.2010457

Buckley, S. J., Ringdal, K., Naumann, N., et al., 2019. LIME: Software for 3-D Visualization, Interpretation, and Communication of Virtual Geoscience Models. *Geosphere*, 15 (1): 222–235. https://doi.org/10.1130/GES02002.1

Chen, S. F., Wilson, C. J. L., Luo, Z. L., et al., 1994. The Evolution of the Western Sichuan Foreland Basin, Southwestern China. *Journal of Southeast Asian Earth Sciences*, 10(3/4): 159–168. https://doi.org/10.1016/0743-9547(94)90016-7

Chesley, J. T., Leier, A. L., White, S., et al., 2017. Using Unmanned

Aerial Vehicles and Structure-from-Motion Photogrammetry to Characterize Sedimentary outcrops: An Example from the Morrison Formation, Utah, USA. *Sedimentary Geology*, 354: 1–8. https://doi.org/10.1016/j.sedgeo.2017.03.013

Colomina, I., Molina, P., 2014. Unmanned Aerial Systems for Photogrammetry and Remote sensing: A Review. *ISPRS Journal of Photogrammetry and Remote Sensing*, 92: 79 – 97. https://doi.org/10.1016/j.isprsjprs.2014.02.013

Cross, N. E., Cunningham, A., Cook, R. J., et al., 2009. Three-Dimensional Seismic Geomorphology of a Deep-Water Slope-Channel system: The Sequoia Field, Offshore West Nile Delta, Egypt. *AAPG Bulletin*, 93(8): 1063–1086. https://doi.org/10.1306/05040908101

Dai, J. X., Ni, Y. Y., Wu, X. Q., 2012. Tight Gas in China and Its Significance in Exploration and Exploitation. *Petroleum Exploration and Development*, 39(3): 277 – 284. https://doi. org/10.1016/S1876-3804(12)60043-3

Du, J. H., He, H. Q., Yang, T., et al., 2014. Progress in China's Tight Oil Exploration and Challenges. *China Petroleum Exploration*, 19 (1): 1 – 9. https://doi. org/10.3969/j. issn. 1672-7703.2014.01.001 (in Chinese with English Abstract)

Duan, W. S., 2021. Exploration potential and favorable direction of tight gas in Middle Jurassic Xiashaximiao Formation in Sichuan Basin. *Petroleum Geology & Experiment*, 43(3): 424 – 431 (in Chinese with English Abstract)

Fabuel-Perez, I., Hodgetts, D., Redfern, J., 2009. A New Approach for Outcrop Characterization and Geostatistical Analysis of a Low-Sinuosity Fluvial-Dominated Succession Using Digital Outcrop models: Upper Triassic Oukaimeden Sandstone Formation, Central High Atlas, Morocco. *AAPG Bulletin*, 93(6): 795–827. https://doi.org/10.1306/02230908102

Fan, Y., 2022. Progress and Development Direction for Key Well Engineering Technology in Tight Sandstone in Shaximiao Famation, Sichuan Basin. *Drilling and Production Technology*, 45 (6): 48–52 (in Chinese with English Abstract)

Fang, R., Jiang, Y. Q., Chen Q., 2023. Sedimentary Characteristics of Jurassic Shaximiao Formation in Wubaochang Area, Northeastern Sichuan Basin. *Lithologic Reservoirs*, 35(2): 47 – 58 (in Chinese with English Abstract)

Hayat, S., Yanmaz, E., Muzaffar, R., 2016. Survey on Unmanned Aerial Vehicle Networks for Civil Applications: A Communications Viewpoint. *IEEE Communications Surveys & Tutorials*, 18(4): 2624 – 2661. https://doi. org/10.1109/COMST.2016.2560343

Huang, D., Li, Y. C., Liu, M., et al., 2017. Reservoir Features and Exploration Potential of the 1st Member of Shaximiao Formation of Middle Jurassic in Central Sichuan Basin. *China Petroleum Exploration*, 22(2): 44 – 49. https://doi. org/10.3969/j. issn. 1672-7703.2017.02.005 (in Chinese with English Abstract)

Ji, Y. L., Wu, S. H., Zhou, Y., et al., 2013. Radiational Bedding in Sandstone and Analysis of Its Origin in Dongyangshugou Section of Luanping, Hebei Province. *Journal of Palaeogeography*, 15(1): 43 – 48 (in Chinese with English Abstract)

Jia, A. L., Guo, J. L., He, D. B., 2007. Perspective of Development in Detailed Reservoir Description. *Petroleum Exploration and Development*, 34(6): 691 – 695. https://doi. org/10.3321/j. issn: 1000-0747.2007.06.010 (in Chinese with English Abstract)

Jia, C. Z., Zou, C. N., Li, J. Z., et al., 2012. Assessment Criteria, Main Types, Basic Features and Resource Prospects of the Tight Oil in China. *Acta Petrolei Sinica*, 33(3): 343–350. https://doi. org/10.3969/j. issn. 1673-8926.2011.04.005 (in Chinese with English Abstract)

Jin, Z. K., Yang, Y. X., Shang, J. L., et al., 2014. Sandbody Architecture and Quantitative Parameters of Single Channel Sandbodies of Braided River: Cases from Outcrops of Braided River in Fukang, Liulin and Yanan Areas. *Natural Gas Geoscience*, 25(3): 311–317 (in Chinese with English Abstract)

Liang, B., Liu, Y. G., Shao, Y. L., et al., 2022.3D Quantitative Characterization of Fractures and Cavities in Digital Outcrop Texture Model Based on Lidar. *Energies*, 15(5): 1627. https://doi.org/10.3390/en15051627

Liang, D. G., Ran, L. H., Dai, D. S., et al., 2011. A re-Recognition of the Prospecting Potential of Jurassic Large-Area and Non-Conventional Oils in the Central-Northern Sichuan Basin. *Acta Petrolei Sinica*, 32(1): 8–17. https://doi.org/10.3969/j.issn.1002-302x.2010.01.008 (in Chinese with English Abstract)

Lin, C. Y., Sun, T. B., Dong, C. M., et al., 2013. Fine Characterization of Remaining Oil Based on a Single Sand Body in the High Water Cut Period. *Acta Petrolei Sinica*, 34(6): 1131–1136. https://doi. org/10.7623/syxb201306012 (in Chinese with English Abstract)

Liu, B. J., Xie, J., Zhang, J. L., 2004. Present Situation and Advance of Remaining Oil Research Technology in China. *Northwestern Geology*, 37(4): 1–6 (in Chinese with English Abstract)

Liu, J. L., Yin, W., Ji, Y. L., et al., 2018. Sequence Architecture and Sedimentary Characteristics of a Middle Jurassic Incised Valley, Western Sichuan Depression, China. *Petroleum Science*, 15(2): 230–251. https://doi.org/10.1007/s12182-017-0211-0

Ma, X. H., Zheng, D. W., Shen, R. C., et al., 2018. Key Technologies and Practice for Gas Field Storage Facility Construction of Complex Geological Conditions in China. *Petroleum Exploration and Development*, 45(3): 507 – 520. https://doi. org/10.1016/S1876-3804(18)30056-9

Ma, Y. S., Cai, X. Y., Zhao, P. R., 2018. China's Shale Gas Exploration and Development: Understanding and Practice. *Petroleum Exploration and Development*, 45(4): 589–603. https://doi.org/10.1016/S1876-3804(18)30065-X

Marques, A., Horota, R. K., de Souza, E. M., et al., 2020. Virtual and Digital Outcrops in the Petroleum industry: A Systematic Review. *Earth-Science Reviews*, 208: 103260. https://doi. org/10.1016/j.earscirev.2020.103260

Moore, A. J., Upchurch, P., Barrett, P., 2020. Osteology of Klamelisaurus Gobiensis (Dinosauria, Eusauropoda) and the Evolutionary History of Middle – Late Jurassic Chinese Sauropods. *Journal of Systematic Palaeontology*, 18(16): 1299–1393. https://doi.org/10.1080/14772019.2020.1759706

Nesbit, P. R., Hubbard, S. M., Daniels, B. G., et al., 2021. Digital re-Evaluation of Down-Dip Channel-Fill Architecture in Deep-Water Slope Deposits: Multi-Scale Perspectives from UAV-SfM. *The Depositional Record*, 7(3): 480 – 499. https://doi. org/10.1002/dep2.137

Nieminski, N. M., Graham, S. A., 2017. Modeling Stratigraphic Architecture Using Small Unmanned Aerial Vehicles and Photogrammetry: Examples from the Miocene East Coast Basin, New Zealand. *Journal of Sedimentary Research*, 87(2):

126–132. https://doi.org/10.2110/jsr.2017.5

Osman, M., Abdullatif, O., Al-Farhan, M., 2017. Workflow of Integration of Digital Outcrop Modeling and Sedimentology of the Early Triassic Upper Khartam Member of Khuff Formation, Central Saudi Arabia. *Arabian Journal of Geosciences*, 10(14): 297. https://doi.org/10.1007/s12517-017-3082-1

Pickel, A., Frechette, J. D., Comunian, A., et al., 2015. Building a Training Image with Digital Outcrop Models. *Journal of Hydrology*, 531: 53 – 61. https://doi. org/10.1016/j. jhydrol.2015.08.049

Qiu, Y. N., Chen, Z. Q., Ju, J., et al., 1983. Discussion on the Development-Geological Classification of Oil Reservoirs in China. *Petroleum Exploration and Development*, 10(5): 35 – 48 (in Chinese with English Abstract)

Sahoo, H., Gani, N. D., 2015. Creating Three-Dimensional Channel Bodies in LiDAR-Integrated Outcrop characterization: A New Approach for Improved Stratigraphic Analysis. *Geosphere*, 11 (3): 777–785. https://doi.org/10.1130/GES01075.1

Szarawarska, E., Huuse, M., Hurst, A., et al., 2010. Three-Dimensional Seismic Characterisation of Large-Scale Sandstone Intrusions in the Lower Palaeogene of the North Sea: completely Injected vs. *in situ* Remobilised Sandbodies. *Basin Research*, 22(4): 517–532. https://doi.org/10.1111/j.1365-2117.2010.00469.x

Wang, C. S., Dai, J. G., Zhao, X. X., et al., 2014. Outward-Growth of the Tibetan Plateau during the Cenozoic: A Review. *Tectonophysics*, 621: 1 – 43. https://doi. org/10.1016/j. tecto.2014.01.036

Wang, Z. C., Zou, C. N., Tao, S. Z., et al., 2004. Analysis on Tectonic Evolution and Exploration Potential in Dabashan Foreland Basin. *Acta Petrolei Sinica*, 25(6): 23 – 28 (in Chinese with English Abstract)

Wen, H. G., Zheng, R. C., Ye, T. R., et al., 2005. High Resolution Sequence Stratigraphy of the Lowershaximiao Formation in the Foreland Basin of micang-Daba Mountain. *Journal of Mineralogy and Petrology*, 25(1): 83 – 90. https://doi. org/ 10.19719/j. cnki. 1001-6872.2005.01.016 (in Chinese with English Abstract)

Wu, C. Y., Liu, B. J., Wang, D. F., et al., 1981. Patterns of Sedimentary Facies of Clastics in China. *Acta Petrolei Sinica*, 2 (4): 1–10 (in Chinese with English Abstract)

Wu, S. H., Yue, D. L., Liu, J. M., et al., 2008. Study on Hierarchical Modeling of Reservoir Configuration of Underground Ancient River Channel. *Science in China Series D*, 38(S1): 111–121 (in Chinese with English Abstract)

Xia, W. J., Li, X. H., Yi, Z. Q., 1984. The Burial Environment of Dinosaur Fauna in Lower Shaximiao Formation of Middle Jurassic at Dashanpu, Zigong, Sichuan. *Journal of Chengdu University of Technology* (*Science & Technology Edition*), 11 (S2): 46–59, 68–69 (in Chinese with English Abstract)

Yan, Y. M., Liang, Y. T., Zhang, H. R., et al., 2019. A Two-Stage Optimization Method for Unmanned Aerial Vehicle Inspection of an Oil and Gas Pipeline Network. *Petroleum Science*, 16(2): 458 –468. https://doi.org/10.1007/s12182-019-0305-y

Yang, X. F., Wang, X. Z., Zhang, S. N., et al., 2014. Sedimentary Characteristic and Oilsands Prediction in the Upper Shaximiao Formation, Houba Area, Northwestern Sichuan Basin. *Geological Science and Technology Information*, 33(3): 112–117 (in Chinese with English Abstract)

Yang, X. P., Zhao, W. Z., Zou, C. N., et al., 2007. Origin of Low-Permeability Reservoir and Distribution of Favorable Reservoir. *Acta Petrolei Sinica*, 28(4): 57–61. https://doi.org/10.3321/j.issn: 0253-2697.2007.04.011 (in Chinese with English Abstract)

Yin, S. L., Chen, G. Y., Liu, Z. L., et al., 2018. 3D Digital Outcrop Characterization Technology Based on Unmanned Aerial Vehicle Oblique Photography. *Acta Sedimentologica Sinica*, 36 (1): 72 – 80. https://doi. org/10.3969/j. issn. 1000-0550.2018.009 (in Chinese with English Abstract)

Yin, T. J., Zhang, C. M., Zhao, H. J., et al., 2001. Remaining Oil Distribution Prediction Based on High-Resolution Sequence Stratigraphy. *Petroleum Exploration and Development*, 28(4): 79 –82 (in Chinese with English Abstract)

Yu, H. Y., Liu, J. L., Hao, Y. Q., et al., 2019. Sand-Body Distribution and Superposed Patterns of Alluvial Deposits in the Middle Jurassic in the Piedmont Zone of the Longmen Mountain Trust Belt. *Geological Journal of China Universities*, 25(3): 389–400. https://doi. org/10.16108/j. issn1006-7493.2018099 (in Chinese with English Abstract)

Yu, X. H., Wang, D. F., Zheng, J. M., et al., 1994.3-D Extension Models of Braided Deltaicsandbody in Terrestrial Facies: an Observation on Deposition of Modern Deltas in Daihai Lake, Inner Mongolia. *Acta Petrolei Sinica*, 15(1): 26 – 37 (in Chinese with English Abstract)

Yue, D. L., Li, W., Wang, W. R., et al., 2019. Analyzing the Architecture of Point Bar of Meandering Fluvial River Using Ground Penetration radar: A Case Study from Hulun Lake Depression, China. *Interpretation*, 7(2): T437 – T454. https://doi. org/10.1190/INT-2018-0144.1

Zeng, H. L., Zhu, X. M., Zhu, R. K., et al., 2012. Guidelines for Seismic Sedimentologic Study in Non-Marine Postrift Basins. *Petroleum Exploration and Development*, 39(3): 295–304. https: //doi.org/10.1016/S1876-3804(12)60045-7

Zhang, L. F., Pan, M., Li, Z. L., 2020. 3D Modeling of Deepwater Turbidite Lobes: A Review of the Research Status and Progress. *Petroleum Science*, 17(2): 317 – 333. https://doi. org/10.1007/ s12182-019-00415-y

Zhang, X. J., Wu, D., Fu, M. Y., et al., 2022. Controls of Sandstone Architecture on Hydrocarbon Accumulation in a Shallow-Water Delta from the Jurassic Shaximiao Formation of the Western Sichuan Basin in China. *Energy Reports*, 8: 6068–6085. https:// doi.org/10.1016/j.egyr.2022.04.001

Zhao, W. Z., He, D. F., Chi, Y. L., et al., 2001. Major Characteristics and Exploration Technology of multi-Source Petroleum Systems in China. *Acta Petrolei Sinica*, 22(1): 6 – 13 (in Chinese with English Abstract)

Zou, C. N., Zhang, G. Y., Tao, S. Z., et al., 2010. Geological Features, Major Discoveries and Unconventional Petroleum Geology in the Global Petroleum Exploration. *Petroleum Exploration and Development*, 37(2): 129 – 145. https://doi. org/ 10.1016/S1876-3804(10)60021-3